NDT-CE 2022 - The International Symposium
on Nondestructive Testing in Civil Engineering
Zurich, Switzerland, August 16-18, 2022

Sorting of construction and demolition waste by combining LIBS with NIR spectroscopy

Tim KLEWE[1*], Tobias VÖLKER[1], Jenny GÖTZ[2], Mirko LANDMANN[2], Gerd WILSCH[1], Sabine KRUSCHWITZ[1,3]

[1] Bundesanstalt für Materialforschung und -prüfung (BAM), Berlin, Germany
[2] Institut für Angewandte Bauforschung Weimar gGmbH, Weimar, Germany
[3] Technische Universität Berlin, Berlin, Germany
*Corresponding author, e-mail address: *tim.klewe@bam.de*

More info about this article: http://www.ndt.net/?id=27220

Abstract
In a joint project of partners from industry and research, the automated recycling of construction and demolition waste (CDW) is investigated and tested by combing laser-induced breakdown spectroscopy (LIBS) and near-infrared (NIR) spectroscopy. Joint processing of information (data fusion) is expected to significantly improve the sorting quality of various materials like concrete, main masonry building materials, organic components, etc., and may enable the detection and separation of impurities such as SO_3-cotaining building materials (gypsum, aerated concrete, etc.). The project focuses primarily on the Berlin site to analyze the entire value chain, minimize economic/technological barriers and obstacles at the cluster level, and sustainably increase recovery and recycling rates.
First measurements with LIBS and NIR spectroscopy show promising results in distinguishing various material types and indicate the potential for a successful combination. In addition, X-ray fluorescence (XRF) spectroscopy is being performed to obtain more information about the quantitative elemental composition of the different building materials. Future work will apply the developed sorting methodology in a fully automated measurement setup with CDW on a conveyor belt.

Keywords: NDT, material classification, recycling, circular economy, LIBS

1 Introduction

Closed material cycles and unmixed material fractions are required to achieve high recovery and recycling rates in the building industry. In CDW recycling, the preference to date has been to apply simple but proven techniques to process large quantities of construction rubble in a short time. This contrasts with the increasingly complex composite materials and structures in the mineral building materials industry. Manual sorting involves many risks and dangers for the executing staff and is merely based on obvious, visually detectable differences for separation. An automated, sensor-based sorting of these building materials could complement or replace this practice to improve processing speed, recycling rates, sorting quality, and prevailing health conditions.
Through the installation of sensor-based single particle sorting devices in building materials recycling, the individual components of the heterogeneous bulk materials could be identified and converted into single-sort material fractions in subsequent processes. In this context, the performance limits of the current sensor techniques as well as economic aspects must be considered. According to the current state of art, only coarser aggregates can be sorted technically and economically with this technology. Current investigations on sensor-based sorting technologies for CDW are based on the analysis of the visual (VIS) and/or the near-infrared (NIR) spectrum [1].
The aim is to detect and sort out foreign materials and impurities before processing. So far, no pre-screening technologies have been used in processing of CDW. However, this is necessary

2022 The Authors. Published by NDT.net under License CC-BY-4.0 https://creativecommons.org/licenses/by/4.0/

to prevent further spreading of undesirable materials in recyclable material streams. This applies in particular to sulphate-containing building materials, such as gypsum plasters.
A current research project with the acronym “LIBS-ConSort” aims to sort mineral CDW using laser-induced breakdown spectroscopy (LIBS) in combination with VIS/NIR spectroscopy. It is expected that the extension of established camera-based techniques will improve the reliability of sorting different groups of building materials. To emphasize this outlook, this study focuses on preliminary results of using LIBS alone to classify common CDW representatives, and provides initial examples of NIR spectra. The quantitative elemental composition of various building materials is further analyzed with X-ray fluorescence (XRF) spectroscopy.

2 Methods

2.1 Building Material Samples

To investigate the capability of LIBS to discriminate different building materials, several samples were gathered, which are listed in Table 1. The eight material groups, comprising a total of 91 samples, are exemplary shown in Figure 1. Due to the present project progress, XRF and NIR spectroscopy are at first performed on individual subsets of 41 and 10 samples, respectively.
Within the data set, 47 out of 91 samples were already known and labeled. The remaining 44 samples were collected from recycling companies in the region of Berlin, Germany. Due to the lack of labels for these samples, a majority vote was conducted by three experts who assigned a material group to each sample.

Table 1: Variety and number of building materials examined with LIBS, XRF and NIR spectroscopy.

	Number of specimens		
Material group	**LIBS**	**XRF**	**NIR**
Aerated concrete	6	4	1
Asphalt	2	-	-
Brick	42	28	4
Concrete/Mortar	14	1	1
Light concrete	5	4	1
Natural stone	2	-	-
Plaster	7	-	2
(Lime) Sandstone	13	4	1

2.2 LIBS Measurements, Pre-processing and Classification

Measurements were performed on the samples from Table 1 using the commercial LIBS instrument “concreteLIBS” from SECOPTA analytics GmbH. Nd:YAG laser (1064 nm) was used at a pulse energy of 1 mJ, puls width of 1.5 ns and a pulse repetition rate of 400 Hz. The detection of the emitted plasma emission was performed with a set four compact spectrometer covering the wavelength range of 250 nm - 940 nm with spectral resolution of approximate 0.1 nm. An area of 20 mm x 20 mm was examined on each sample at a lateral resolution of 0.5 mm (Figure 1). The entire dataset contains 152,971 spectra with 7774 data points per spectrum. It forms the basis for the following pre-processing and training of a classifier.

Figure 1: Exemplary pictures for each material group and the measuring area of LIBS on a concrete sample (blue square).

Before extracting discriminating features, sample-related outliers in terms of total spectral intensity were removed from the dataset. Therefore, any spectrum below 75 % of the maximum total sample intensity (calculated by a trapezoidal rule integral) was discarded. This was done to exclude measurements with insufficient laser focus due to possible sample roughness or unevenness. Thus, the dataset was reduced to 75,591 spectra (roughly 50 %).
To generate an input vector for the following classification task, the spectral line intensities of ten different elements are extracted from each spectrum (see Table 2). For this purpose, a baseline correction is performed for each spectral line, followed by a calculation of the integral line intensity. In addition to the ten extracted element features, the first two principal components were calculated by a Principal Component Analysis (PCA) over all standardized spectra.

Table 2: Chemical elements and their center wavelength in the LIBS spectrum used for material classification and assignment of the corresponding building material class.

Element	Wavelength in nm
Iron (Fe)	259.94
Magnesium (Mg)	285.21
Silicon (Si)	288.16
Aluminum (Al)	309.27
Calcium (Ca)	315.89
Titanium (Ti)	334.94
Potassium (K)	796.90
Sodium (Na)	818.33
Oxygen (O)	844.64
Sulfur (S)	921.29

The reduced data matrix of 75,591 × 12 (number of spectra × number of features extracted) is labeled according to the material groups in Table 1, which also define the eight desired output classes for the supervised training process. Here, a random forest classifier, included in the scikit-learn library (python) [2], is used in standard configuration (default parameters only).

To avoid the scenario of overfitting and to simulate a realistic classification problem of unknown samples, a cross validation is performed as follows: According to the total number of samples, we define 91 different training data sets, each excluding one individual sample, which in turn serves as the respective test data. This shall test the capability of a trained classifier to recognize an unknown sample. An exclusively correct classification on known samples and poor accuracies on others would indicate overfitting [3]. Therefore, 91 models are trained and applied on their respective unkown test sample to predict the material group. Instead of presenting 91 individual results, the achieved accuracies are accumulated and evaluated in one confusion matrix (see later Figure 4).

2.3 NIR spectroscopy

A subset of ten building materials (Table 1) was measured with the hyperspectral imaging (HSI) line cameras KUSTA1.7 and KUSTA2.2 from LLA instruments GmbH to provide first insights into the different reflectance spectra of CDW representatives. The former measures the NIR range from 0.95 µm to 1.7 µm, while the latter covers the short-wave infrared (SWIR) range from 1.6 µm to 2.2 µm.
All samples were measured in a single recording for each camera, which is exemplary shown for the KUSTA 2.2 in Figure 2. From those, 5 px x 5 px regions of interest (ROI) were extracted to calculate the material specific mean reflectance in each ROI.

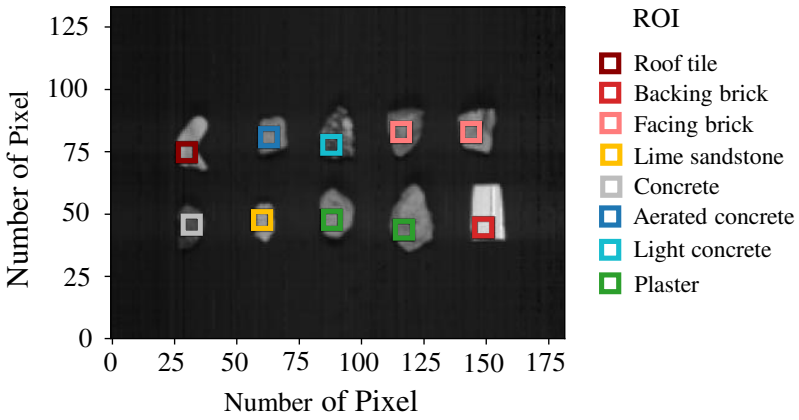

Figure 2: Recorded grayscale image (camera: KUSTA 2.2) with applied ROIs for mean reflectance calculation.

2.4 XRF

To obtain additional information about the elemental composition, X-ray fluorescence analysis (XRF) was performed. For this purpose, 41 single-variety samples were analyzed (Table 1).
The available materials were in particle sizes of 4 mm - 8 mm, so for the analysis 20 g of sample material were ground to powder with largest grain size of 63 µm. Concrete samples were dried at 40 °C in a vacuum oven and subsequently ignited at 950 °C for determining the loss on ignition (LOI). Brick samples were treated at 110 °C and 1,025 °C respectively for obtaining the LOI. Then, fusion beads were prepared by mixing the ignited sample with a lithium borate flux from Claisse in a ratio 1:10 and fused for 20 min. XRF analysis was carried out on a WD-XRF instrument ZSX Primus IV from Rigaku (Rh anode, max. 4 kW) in vacuum atmosphere applying the fundamental parameter method to investigate the chemical composition from fluorine to uranium.

3 Results

3.1 Classification by LIBS

A general overview of the measured LIBS data set is given in Figure 3, which shows the standardized mean intensities and standard deviations of the twelve extracted element features for each material group. The figure gives a first impression of the feature-based separability of the examined samples and reveals characteristic distributions between the material groups.
The first striking feature is the relatively high standard deviation for certain features and material groups. This is due to the heterogeneous samples such as concrete/mortar, light concrete, and natural stone, which may contain different materials and thus also different element concentrations within one measurement area.
The second point to focus on is the separability of different material groups. Asphalt has comparatively low intensities for each feature and may therefore be classified better than plaster, light concrete, or sandstone, whose intensity distributions resemble one another. Relatively high intensities are also observed for bricks, especially for the first four features Fe, Mg, Si and Al. This may also indicate good detectability within the data set.

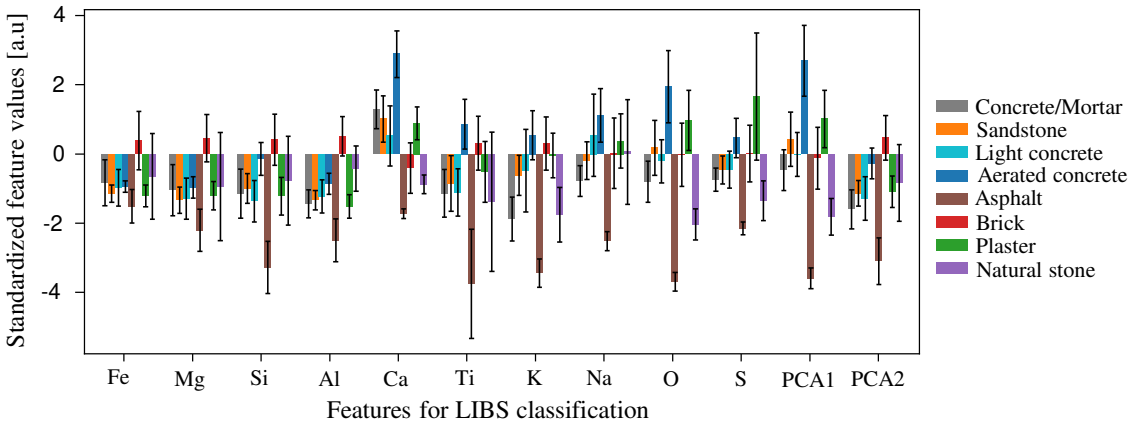

Figure 3: Standardized mean intensities (color bars) and standard deviations (black lines) of the extracted features for each material group.

The distribution discussed provide suitable information to obtain first indications of the classification accuracies archived for each material group, which are shown in form of a confusion matrix in Figure 4 a). The scores are given in the range from 0 to 1, standing for 0 % to 100 % of the respective test data. Here, the diagonal includes the most meaningful values and shows accuracies between 5 % and 99 %. Asphalt and brick can be classified best, which is in accordance with the good separability concerning their feature distribution discussed in Figure ***3***. Also, concrete/mortar, sandstone and aerated concrete achieved satisfying accuracies above 80 %. With a score of 64 %, plaster is often confused with sandstone or light concrete, the latter being correctly classified in only half of measurements. This could result from the heterogeneous structure discussed above, leading to comparatively higher deviations for the concerned features. Natural stone (5 % accuracy) was mostly recognized as brick. Here, the data set contained only two individual samples, which is insufficient for machine learning. These approaches generally require a large and diverse data basis to achieve accurate and robust classification results. However, asphalt, which was as well only represented by two samples,

showed an almost perfect classification result. Here, the distinctive distribution of relatively low intensities for every feature resulted in a high score. Unfortunately, it is not yet possible to say whether these findings are representative of the material group in question. Further samples of each class, especially for those that are still underrepresented, will provide further insights into their separability.
So far, each individual LIBS spectrum within a measurement has been classified separately. With a sorting approach, the recognition of an entire sample is of greater importance, so Figure ***3*** b) shows the scores obtained based on a sample majority vote. This means that each sample was classified according to the material group that was estimated most within the measurement area. In this way, the accuracies for each class, with the exception for plaster, increased significantly.
Due to the possible contamination by other materials, plaster is considered a critical material to be excluded in the early stages of the recycling process. Here, the combination of LIBS with NIR spectroscopy might enable higher detection rates.

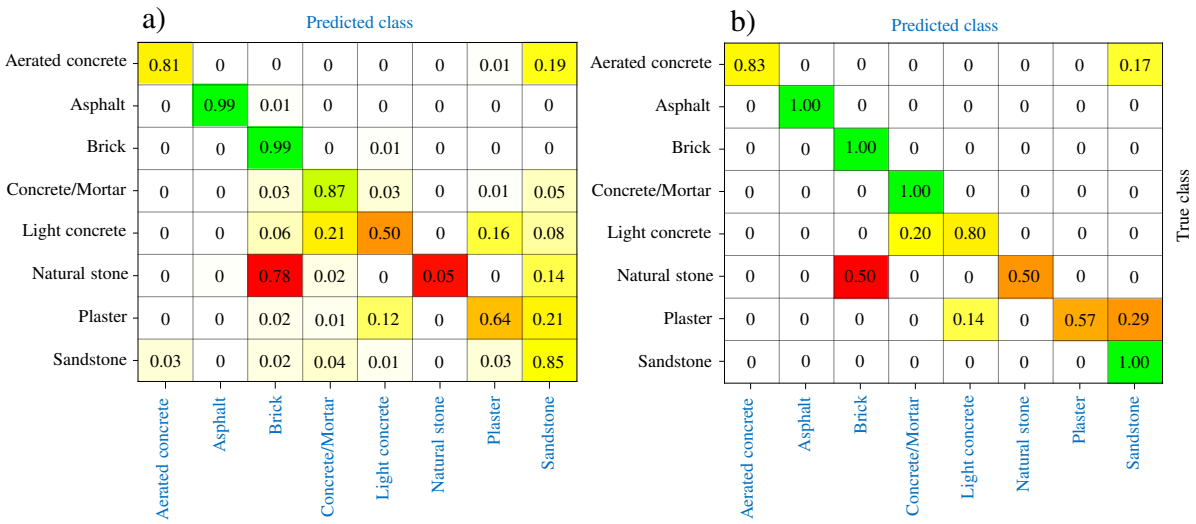

Figure 4: Confusion matrixes of the performed cross validation, showing the achieved classification accuracies for each single LIBS spectrum (a) and with sample related majority vote (b). Rows contain the true classes (black) and columns the predicted classes (blue).

3.2 NIR spectroscopy

The mean reflectance in the NIR and SWIR range for representatives of each considered material group is given in Figure 5. Here, every spectrum is normalized to its individual maximum for a proper comparison of the degrees of absorption. Generally, NIR spectra contain information about the major hydrogen bonds, i.e., C–H, O–H and N–H [5]. This means, that all molecules containing hydrogen show dominant absorption in the range of approx. 1.35 µm to 1.55 µm and in the range of 1.85 µm and 2.05 µm. Except for the brick materials, all other types caused such a measurable decrease in the reflectance signal. They differ mainly in the degree of absorption and the associated wavelength of the reflection minimum. Plaster, which was pointed out as a crucial material in the previous section, shows comparatively strong absorption patterns for a generally broader wavelength range. This might help to compensate for the poorer classification accuracy by the sole use of LIBS, if both measurement techniques are combined.

Since the NIR investigation was only conducted on a small subset, the findings still need to be checked and validated against a larger data set. Therefore, further measurements and subsequent data fusion with LIBS are planned.

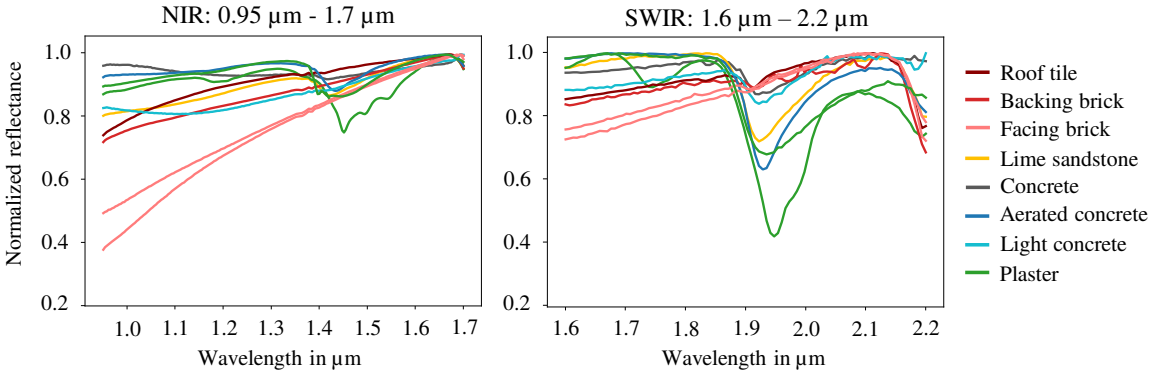

Figure 5: Normalized mean reflectance of the investigated materials in the NIR (left) and SWIR (right) regions.

3.3 XRF analysis

The XRF results are shown in Figure 6. The following oxides were considered in the evaluation: SiO_2, Al_2O_3, Fe_2O_3, CaO, MgO, Na_2O, K_2O, TiO_2, and SO_3.
For a first overview, the mean concentrations with their corresponding standard deviations are presented in Figure 6 a), which shows the main differences between the materials in terms of their chemical compositions. SiO_2 has the highest concentrations across all materials analyzed (40-83 wt.%), while SO_3 has concentrations close to 0 wt.% except for lightweight concrete (1 wt.%). Some material specific elements could be observed, like CaO, which made up to 32 wt.% in aerated concentrates or NaO_2 (up to 5.2 wt.%) in lightweight concrete. No clear differences can be defined based on the other oxides in Figure 6 a).

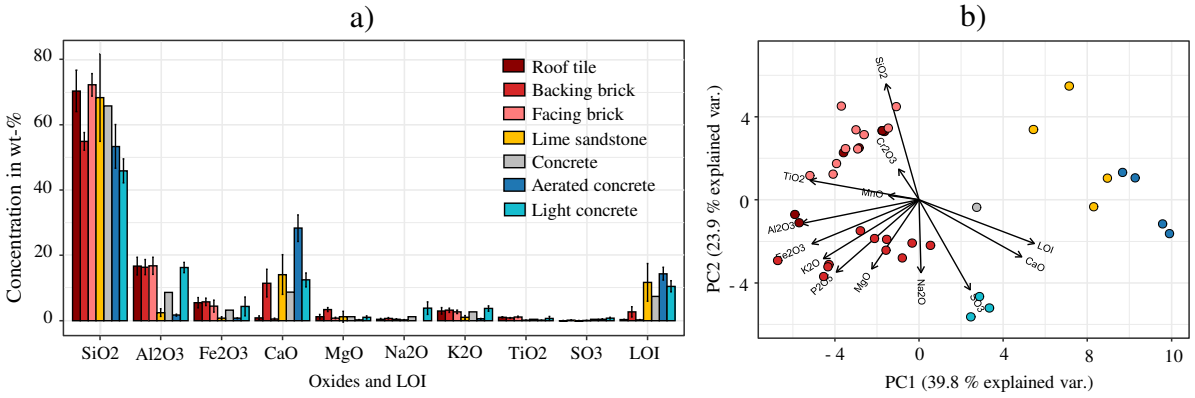

Figure 6: a) Overview of the chemical composition (XRF data) of the different materials. Mean concentration values (colored bars) with standard deviations (black lines) are shown. b) PCA analysis based on the chemical composition for different materials (colored dots) and the influence of the oxides (arrows).

To gain better insight into the data, a PCA is performed, presented in Figure 6 b), where the investigated samples cluster together according to their chemical composition. We observe 2 clusters: brick (to the left) and concrete-sandstone-aerated concrete (to the right). Only the lightweight concrete sample cannot be clearly assigned and forms its own cluster (in this representation). As expected, samples of the same materials are also cluster together.
PC1 represents the gradient of Al_2O_3 or TiO_2 to CaO, while PC2 is associated with the gradient SiO_2 to Na_2O. Hence, SiO_2 rich samples have positive values for PC1 and all Na_2O rich samples have negative ones. The same holds for CaO rich samples (positive values for PC1) and Al_2O_3 rich samples (negative values for PC1). The clustering is in accordance with the three-phase diagram SiO_2-flux (Fe_2O_3+CaO+MgO+K_2O+Na_2O)-Al_2O_3 of Müller [4].

4 Summary and Conclusion

In this study, preliminary results of the classification of different groups of building materials by using LIBS were presented and insights into first investigations with NIR and XRF spectroscopy were given. Spectral information from 91 different CDW representatives were collected using LIBS, from which twelve features were extracted. These features, containing ten element-specific information and the first two principal components, were used to train numerous random forest classifiers, which were then applied to unknown test samples.
Brick, asphalt, concrete/mortar, sandstone, and aerated concrete achieved satisfying accuracies, ranging from 81 % - 99 %. Plaster, light concrete, and natural stone showed lower accuracies of 64 %, 50 %, and 5 %, respectively. In the case of light concrete and natural stone, the higher heterogeneity, similar spectral properties, and the low number of samples within the data set may explain the poor results.
Since the presented work outlines only the first results of an ongoing research project, the achieved accuracies can generally be considered promising. It is expected that the underlying data set will grow significantly though the collection of further samples and will serve as a solid basis for the planned methodological combination with VIS/NIR-cameras. Here, first results of NIR spectroscopy show good potential to provide valuable information to further increase sorting quality.
To gain further insight into the elemental composition of various building materials, XRF analysis was performed. Here, the generally good separability of brick materials, which was also achieved in the LIBS data, was confirmed by principal component analysis. The overlapping compositions of sandstone and aerated concrete were also found by both LIBS and XRF.
Future works will investigate the influence of different moisture contents and surface contamination (dust, soil) on the individual measurement procedure as well as on the classification results. The results will help to plan effective pre-processing of CDW in the industrial prototype, which may include washing of samples prior to their identification.

Acknowledgements

Financial support by the Federal Ministry for Education and Research in the framework of ReMin (grant number 255 033R259C) in Germany is greatly appreciated.

References

[1] A. Müller, ‚Erschließung der Ressourceneffizienzpotentiale im Bereich der Kreislaufwirtschaft Bau‘, Project report in the research program Zukunft Bau, Bundesinstitut für Bau-, Stadt- und Raumforschung im Bundesamt für Bauwesen und Raumordnung, 2016

[2] F. Pedregosa, G. Varoquaux, A. Gramfort, V. Michel, B. Thirion, O. Grisel, M. Blondel, P. Prettenhofer, R. Weiss, V. Dubourg, J. Vanderplas, A. Passos, D. Cournapeau, M. Brucher, M. Perrot, E. Duchesnay, ‚Scikit-learn: Machine Learning in Python‘. Journal of Machine Learning Research 2011, Vol. 12, pp. 2825–2830, 2011

[3] Dietterich, ‘Overfitting and undercomputing in machine learning.’ ACM computing surveys (CSUR) Vol. 27, No. 3, pp 326-327, 1995

[4] A. Müller, ‚Baustoffrecycling-Entstehung - Aufbereitung - Verwertung.‘ s.l. : Springer Vieweg Wiesbaden, 2018.

[5] M. Manley, ‘Near-infrared spectroscopy and hyperspectral imaging: non-destructive analysis of biological materials.’ Chemical Society Reviews, Vol 43, pp 8200-8214, , 2014